



Research Article

ESTIMATION PERFORMANCE OF SOIL MOISTURE WITH GPS-IR METHOD

Cemali ALTUNTAŞ¹, Nursu TUNALIOĞLU*²

¹*Yildiz Technical University, Dept. of Geomatic Engineering, ISTANBUL; ORCID: 0000-0002-9660-6124*

²*Yildiz Technical University, Dept. of Geomatic Engineering, ISTANBUL; ORCID: 0000-0001-9345-5220*

Received: 11.06.2020 Revised: 08.10.2020 Accepted: 02.12.2020

ABSTRACT

This study aims to retrieve soil moisture from Global Positioning System (GPS) Signal-to-Noise Ratio (SNR) data with varying analysis to compute the best-fitting analyzing methodology. Phase, amplitude, and reflector height, which are SNR-derived interferogram metrics are examined and results are proofed with respect to correlation coefficients compared with in-situ measurements. Here, Soil Moisture Content (SMC) is estimated from SNR data with four data analyzing strategies using Lomb Scargle Periodogram to retrieve dominant frequency as; (1) considering it is four times greater than background noise assuming the reflector height is inconstant in each day, (2) considering it is three times greater than background noise assuming the reflector height is inconstant in each day, (3) assuming the reflector height is constant and median values are used for overall estimations in each day, (4) assuming the reflector height is constant and median values are used in each day. To do that, the GPS Interferometric Reflectometry (GPS-IR) method was implemented to the data of OSOR station, installed in Chile (within the scope of the CAP Andes GPS Network Project carried out by UNAVCO), during 213 days from 01 January 2015 to 31 July 2015. Validation of the estimates is done by the recorded soil moistures from the Oromo Calibration Site in the LAB-net network. Results show that SMC estimated from SNR-derived metrics shows well agreement with in-situ measurements i.e. as the highest correlation of 95%; whilst the second strategy was followed.

Keywords: Global Positioning System Interferometric Reflectometry (GPS-IR), Signal-to-Noise Ratio (SNR), Soil Moisture Content (SMC), Lomb Scargle Periodogram (LSP).

1. INTRODUCTION

Soil moisture is a fundamental component of the hydrological cycle and a key observable variable for optimizing agricultural irrigation management and climatology studies [1-5]. Water content in soil can be expressed as gravimetric or volumetric, where gravimetric water content is the ratio of the mass of water over the mass of dry soil, and volumetric water content is the volume of liquid water per volume of soil [6]. The data gathered for the soil moisture retrieval studies can be either as in-situ measurements collected at many locations or remote sensing methods. The in-situ data is location dependent that provides point-based information. Soil moisture can be retrieved by remote sensing methods that provide consistent observations on a

* Corresponding Author: e-mail: ntunali@yildiz.edu.tr, tel: (212) 383 52 98

global scale. However, the problem with this method is that the short wavelengths used are only sensitive for a few mm depths below the surface [2].

Today, the Global Positioning System (GPS) has been routinely used in many scientific and practical engineering applications where high precision point positioning is needed [7, 8]. As commonly known, if high precision point positioning is required, the signals received by the receiver should be eliminated from the errors or the errors should be modelled. In recent years, a novel approach, which utilizes one of the great error sources of GPS received data, so-called multipath, has been introduced to GPS applications to retrieve surface characteristics where the signal reflects. If the signal transmitted from the satellite follows more than one path for arriving at the receiver, the multipath error raises. To eliminate the multipath effect in carrier phase observable at the estimation step; orbits, atmospheric delays, clocks, and positions should be modelled. However, this unwanted effect has become an effective tool to retrieve the surface characteristics where the receiver is established by the help of recorded Signal-to-Noise Ratio (SNR) data in receiver. The geodetic GPS receivers record carrier phase and pseudorange observables [9]. Besides those, one important quantity is also recorded in the receiver, which is SNR. SNR is an indicator to show the power of the interfered signal formed by direct and reflected signals. One should note that this indirect reflection due to multipath error directly affects the SNR data, such as forming amplitude variations as a function of ground reflectivity and therefore Soil Moisture Content (SMC) [3,10]. The GPS carriers are in L-band (1176.45 MHz (L5), 1227.60 MHz (L2), and 1575.42 MHz (L1) frequencies), which are sensitive to the ground where they reflect. If the signal reflects from the soil, then the SNR data is able to represent the characteristic of soil components. By ground-based GPS studies, the interference of the direct and reflected signals is used. As stated in [11], GPS receiver has been dedicated for soil moisture estimation, which is known as GPS-Interferometric Reflectometry (GPS-IR) [12, 13] or Interference Pattern Technique [14] that can be introduced as a novel microwave remote sensing tool working on L-band.

This study aims to estimate SMC with GPS-IR method while the estimation performances vary with four analyzing strategies of the dominant frequency of SNR data (recorded at OSOR station): (1) considering it is four times greater than background noise assuming the reflector height is inconstant in each day, (2) considering it is three times greater than background noise assuming the reflector height is inconstant in each day, (3) assuming the reflector height is constant and median values are used for overall estimations in each day, (4) assuming the reflector height is constant and median values are used in each day. The validation of the results is provided by in-situ measurements where the soil moisture recorded hourly at a meteorological site (namely, OCS).

2. FUNDAMENTAL OF ESTIMATION FOR SOIL MOISTURE CONTENT

GPS receivers record direct and reflected signals simultaneously. These signals interfere at the antenna phase center of the receiver, where they are collected. SNR, provided by GPS receivers, includes the effect of that interference, i.e., it is modulated by multipath signals. This modulation is observed especially at low elevation angles where the number of reflected signals increases. Assuming that there is only one reflected signal, the SNR equation can be written as given in Eq. 1 [3, 15, 16];

$$SNR^2 = A_d^2 + A_m^2 + 2A_d A_m \cos \Delta\varphi \quad (1)$$

where $\Delta\varphi$ is phase delay, A_d and A_m are the amplitudes of the direct and reflected signals, respectively. Since $A_d \gg A_m$, the contribution of the direct signal to the SNR is eliminated by using a low-order polynomial [12]. As a result, SNR section modulated by the reflected signals remains, which is referred to as dSNR in this paper.

dSNR is a periodic signal that oscillates around zero as a function of the sine of the satellite elevation angle, having an amplitude, a phase, and a frequency. This signal can be expressed by Eq. 2;

$$dSNR = a \cos\left(\frac{4\pi h}{\lambda} \sin E\right) + b \sin\left(\frac{4\pi h}{\lambda} \sin E\right) \tag{2}$$

where λ is the wavelength of the signal, h is the reflector height, E is the satellite elevation angle, a and b are the amplitudes of the cosine and sine components of the signal, respectively. The amplitude of the multipath modulation, A_m , which also means the amplitude of the dSNR, can be calculated with Eq. 3;

$$A_m = \sqrt{a^2 + b^2} \tag{3}$$

and the phase of the multipath modulation, $\Delta\phi$, is as given in Eq. 4:

$$\Delta\phi = \tan^{-1}\left(\frac{b}{a}\right) \tag{4}$$

If the reflector height, h , is unknown, the multipath frequency, f_m , is first calculated using the Lomb-Scargle Periodogram (LSP). Then h is obtained using the Eq. 5;

$$h = \frac{\lambda f_m}{2} \tag{5}$$

After obtaining the reflector height, a and b parameters are estimated by the least squares estimation (LSE) method by using Eq. 2. Then, the amplitude and phase are calculated using Eqs. 3 and 4.

There is a relationship between the strength of the signal reflected from the soil and the soil moisture. As the amount of water content in the soil increases, the signal penetrates the soil less, and it reflects more strongly. Furthermore, a signal reaching dry soil penetrates deeper, while the signal reaching wet soil is reflected closer to the surface. Therefore, depending on the moisture of the soil, the phase of the multipath signal and the reflection depth also change. So, SMC can be retrieved from the amplitude, phase, and reflector depth metrics of GPS-IR.

3. STUDY AREA, EXPERIMENTAL DATA AND ANALYSIS

The study area is the OSOR GPS station, which is established in Chile within the scope of the CAP Andes GPS Network Project carried out by UNAVCO, and its surroundings. The station collected data from June 2010 to October 2015, and it was removed in October 2015. Detailed information about the station can be found in Table 1.

Table 1. Location and Operational Information of OSOR Station

GPS site name	Osorno
Site ID	OSOR
Latitude (WGS84)	40° 35' 49.92" S
Longitude (WGS84)	73° 06' 12.96" W
Receiver / Serial number	LEICA GR10 / 1700241
Earliest data time (UTC)	2010 June 02 20:39
Latest data time (UTC)	2015 October 07 23:59

To verify the estimations obtained from the GPS data, in-situ measurements recording soil moistures are required. The Oromo Calibration Site (OCS) in the LAB-net network was selected for this study, which is the closest site to study area. Both sites have similar climatic and meteorological conditions. Details regarding the soil moisture site are represented in Table 2.

Table 2. Location and Operational Information of OCS Soil Moisture Site

Soil moisture site name	Oromo Calibration Site (OCS)
Latitude (WGS84)	40° 53' 06.07" S
Longitude (WGS84)	73° 06' 31.41" W
Sensor	Campbell CS650
Sensor depth	0.07 m
Earliest data time (UTC)	2014 June 18 01:00
Latest data time (UTC)	2017 September 25 21:59

By examining the data at the stations, an observation period was selected, covering the dry and rainy days, with including a sufficient number of common observations in both sites. Thus, a 213-day period (between 1 January 2015 (DoY: 1) and 1 August 2015 (DoY: 213)) was selected to evaluate the observations.

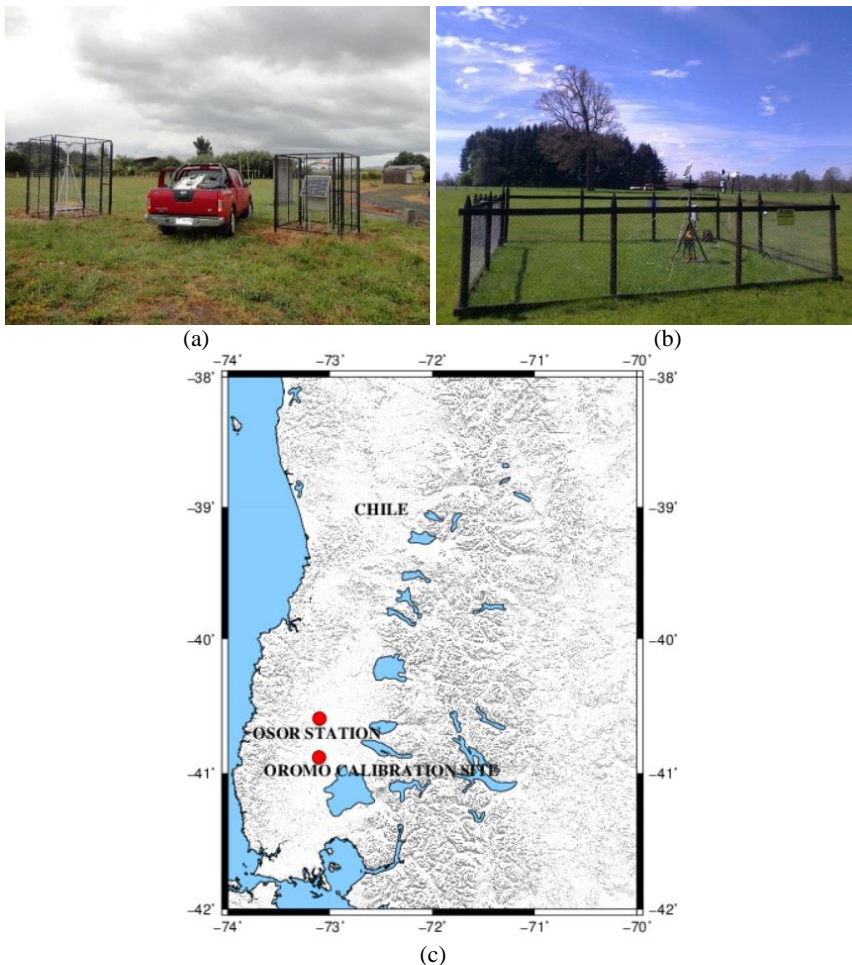


Figure 1. Stations used in the study (a) OSOR GPS site (b) soil moisture sensor at OCS site (c) location map of sites

In the GPS-IR studies carried out so far, it has been shown that the signals coming below 30 degrees elevation angle for geodetic GPS receivers are more affected by the multipath and therefore more modulated. So, in GPS-IR studies, generally, signals coming below 25 or 30 degrees of satellite elevation angle are evaluated. However, unlike these studies, depending on the receiver antenna structure and topography, the multipath effect can be seen in the signals coming from the elevation angles outside the range of 0-30 degrees. Especially when the research aim is to determine soil moisture, higher elevation angles are preferable as they allow the signal to penetrate deeper into the soil than lower ones. Considering the GPS data collected at the OSOR station, it was seen that this is more appropriate to prefer 15-35, and 20-40 degree intervals instead of 0-25 or 0-30 degree intervals.

In this study, only GPS L2 SNR observations were used. Data suitable for analysis were selected manually. Satellites, elevation angle ranges, and azimuth ranges were set according to the signal sections with strong reflection (i.e., dominant sinusoidal signal structure). So, signal sections with the following variables (see, Table 3) were found suitable for evaluation.

Table 3. Predefinition of the data to be used for retrieving soil moisture

Data ID	Satellite	Satellite pass	Elevation angle range (°)		Azimuth range (°)	
			Min.	Max.	Min.	Max.
S2_01	G01	Descending	20	40	0	40
S2_02	G03	Descending	15	35	30	90
S2_03	G04	Descending	20	40	10	60
S2_04	G05	Ascending	20	40	200	260
S2_05	G06	Ascending	20	40	200	260
S2_06	G07	Descending	15	35	90	150
S2_07	G09	Descending	20	40	50	110
S2_08	G13	Descending	20	40	0	40
S2_09	G14	Descending	20	40	100	160
S2_10	G15	Descending	20	40	330	360
S2_11	G16	Ascending	20	40	210	250
S2_12	G17	Descending	20	40	100	160
S2_13	G18	Ascending	20	40	0	50
S2_14	G18	Descending	20	40	110	150
S2_15	G19	Descending	20	40	0	10
S2_16	G22	Ascending	20	40	350	10
S2_17	G23	Descending	20	40	70	140
S2_18	G24	Descending	20	40	0	50
S2_19	G27	Descending	20	40	0	30
S2_20	G28	Ascending	20	40	0	30
S2_21	G31	Ascending	20	40	210	250
S2_22	G32	Descending	15	35	60	120

As can be seen in Table 3, 22 different data sets were selected. The data sets are numbered from 1 to 22 to make it easier to refer to them, and the phrase “S2”, which denotes the L2 SNR, is added in front of these numbers. All of the SNR-derived interferogram metrics, namely amplitude, phase, and reflection depth were investigated and used in the initial studies to determine soil moisture by using the GPS-IR technique. In recent studies, the multipath relative phase has been used more intensively [17-19]. In this study, in order to find the best metric that reflects the soil moisture more accurate, four different parameterizations (referred to as a strategy)

are tested to evaluate the data of the OSOR station. Table 4 summarizes these strategies (denoted as P-0#) with conditions.

Table 4. Analyzing strategies of SNR data collected from OSOR Station

	P-01	P-02	P-03	P-04
Satellite system	GPS	GPS	GPS	GPS
Satellite signal	L2	L2	L2	L2
Strong reflection condition	Max(A) > 4*BN	Max(A) > 3*BN	-	-
Reflector height	Not constant. It is daily estimated.	Not constant. It is daily estimated.	The median of all estimates was taken as constant reflector height.	The median of its estimates was used for each data.
Maximum reflector height (for LSP analysis)	5 m	5 m	-	-
Desired precision (for LSP analysis)	0.01 m	0.01 m	-	-
Minimum elevation angle range	10 degree	10 degree	10 degree	10 degree

In addition to that, to investigate and reveal how strong the relationship between the strategies given in Table 4 and SMC values, estimation rate and correlation coefficient computations are used. Here, the estimation rate (ER) is a ratio computed as given in Eq. 6;

$$ER = \frac{NoED}{NoOD} \tag{6}$$

Where, NoED and NoOD indicate the number of estimation days and number of observation days, respectively.

To represent the statistical relationship between two variables (strategies and SMC), the Pearson correlation coefficient (ρ) is implemented as given in Eq.7 [20];

$$\rho = \frac{\sum xy - n\bar{x}\bar{y}}{(n-1)SD_xSD_y} \tag{7}$$

Here, x and y are the variables, \bar{x} and \bar{y} are the mean values of variables, n is the number of variables, SD is the standard deviation.

4. RESULTS AND DISCUSSION

In P-01 and P-02 processes, the reflector height was estimated daily using LSP, and the amplitude and phase components were estimated with the LSE method using that reflector height. The only difference in these two parameterizations is the coefficient of the strong reflection condition defined depending on the background noise. In P-03 and P-04, reflector height was taken as a known parameter and a constant value was used for all days. While this constant value is the median of all reflector height estimates in P-03, it is the median of the reflector height estimates of each data set in P-04. For example, while the reflector height of 2.45 m is used in P-03 for the data set numbered as S2_17, the reflector height of 2.14 m is used in P-04.

The correlation percentages between the GPS-IR soil moisture estimations made by using P-01 parameterization and the measurements of the soil moisture sensor in the OCS are given in Table 5. The estimation rate values expressing the number of estimated days within the 213-day observation period are also added to the table to represent the compatibility with the condition used in P-01. In addition to these, the median values of the reflector heights estimated from each

data set are also given in Table 5. Moreover, in the following tables (Tables 5-9), the dash line indicates that no positive correlation was found.

Table 5. Correlation percentage of P-01

Data ID	ρ (%)			ER (%)	Median RH (m)
	A	φ	-Refl. Depth		
S2_01	91.31	-	18.52	85.24	2.45
S2_02	74.60	-	53.34	42.86	2.53
S2_03	75.99	81.03	46.72	50.48	2.41
S2_04	84.26	1.24	77.05	42.38	2.43
S2_05	89.03	66.68	64.82	55.24	2.40
S2_06	84.78	40.62	-	36.19	2.62
S2_07	56.59	-	12.74	12.38	2.28
S2_08	88.82	11.37	12.58	77.14	2.56
S2_09	81.99	21.02	-	8.10	2.40
S2_10	74.19	28.24	22.09	73.81	2.47
S2_11	76.57	17.88	-	56.19	2.39
S2_12	29.29	-	24.82	30.48	2.37
S2_13	64.16	44.60	-	42.38	2.45
S2_14	85.15	-	27.72	68.57	2.46
S2_15	88.37	43.02	-	86.67	2.43
S2_16	90.14	28.75	9.60	93.33	2.41
S2_17	82.18	48.79	-	43.81	2.14
S2_18	92.90	64.06	-	71.43	2.47
S2_19	77.45	25.89	9.74	60.95	2.62
S2_20	84.93	4.81	-	60.00	2.59
S2_21	73.52	-	14.78	42.38	2.40
S2_22	54.09	-	56.42	38.10	2.59
Mean	77.29	35.20	32.21	53.55	2.45

According to the results of P-01, mean correlation values between amplitude, phase and reflection depth estimates and OCS measurements were found 77.29%, 35.20% and 32.21%, respectively. The mean estimation rate was found to be 53.55%, i.e., GPS-IR soil moisture estimations could not be made for half of the observation period.

Correlations between GPS-IR soil moisture estimates in P-02 and OCS measurements, estimation rates, and median of the daily estimated reflector heights are given in Table 6.

According to the results of P-02, the mean correlations between amplitude, phase, and reflection depth estimations and OCS measurements were found as 85.54%, 29.71%, and 36.69%, respectively. The estimation rate was found as 88.64% on average. It is seen that using the coefficient “3” instead of “4” in strong signal condition improves the GPS-IR soil moisture estimates made by using amplitude and increases the estimation rate.

Table 6. Correlation percentage of P-02

Data ID	ρ (%)			ER (%)	Median RH (m)
	A	φ	-Refl. depth		
S2_01	89.58	-	19.01	93.33	2.45
S2_02	77.63	-	47.08	90.48	2.54
S2_03	79.35	57.92	-	86.19	2.40
S2_04	88.39	19.27	83.84	90.48	2.47
S2_05	94.43	38.38	67.92	90.48	2.42
S2_06	90.70	28.17	11.87	93.81	2.61
S2_07	88.06	32.18	-	51.43	2.27
S2_08	91.70	5.57	21.25	98.57	2.56
S2_09	75.76	-	-	73.81	2.43
S2_10	71.81	28.23	21.32	99.52	2.47
S2_11	87.61	29.86	48.13	85.71	2.40
S2_12	78.30	6.87	60.20	90.00	2.41
S2_13	87.33	-	-	84.29	2.45
S2_14	89.33	-	28.61	92.38	2.46
S2_15	88.22	39.53	-	93.33	2.43
S2_16	89.36	-	7.08	98.10	2.41
S2_17	85.76	42.53	-	91.90	2.14
S2_18	95.40	64.11	-	97.62	2.47
S2_19	81.90	30.89	-	92.38	2.62
S2_20	91.32	10.64	1.24	93.33	2.59
S2_21	87.82	11.49	37.45	77.62	2.40
S2_22	72.11	-	58.60	85.24	2.60
Mean	85.54	29.71	36.69	88.64	2.45

Correlations between GPS-IR soil moisture estimates made using the parameterization P-03 and a constant reflector height value (2.45 m) and OCS measurements and estimation rates are given in Table 7.

According to the results of P-03, the mean correlation values were found 82.39% for amplitudes, and 78.77% for phase estimations. The average estimation rate was found at 95.71%. In these analysis results, it is seen that the phase estimations, as well as the amplitude estimates, have a high correlation with the OCS measurements, in addition to this; the estimation rate has increased significantly.

Table 7. Correlation percentage of Case P-03

Data ID	ρ (%)		ER (%)
	A	φ	
S2_01	86.72	75.53	94.29
S2_02	75.92	63.99	93.33
S2_03	75.04	85.80	93.81
S2_04	85.55	83.12	93.33
S2_05	87.07	86.63	92.86
S2_06	89.00	79.72	96.67
S2_07	56.61	84.59	93.33
S2_08	92.66	87.37	99.52
S2_09	75.25	73.08	93.33
S2_10	71.92	86.83	100.00
S2_11	86.11	76.75	98.57
S2_12	78.89	83.44	100.00
S2_13	87.47	83.68	97.62
S2_14	89.47	77.63	93.33
S2_15	81.71	83.62	94.29
S2_16	88.71	90.61	98.10
S2_17	86.70	-	92.86
S2_18	94.67	88.82	100.00
S2_19	70.11	51.95	93.81
S2_20	88.02	70.59	94.76
S2_21	89.43	66.61	100.00
S2_22	75.60	73.79	91.90
Mean	82.39	78.77	95.71

The correlation values between the GPS-IR soil moisture estimates using the parameterization P-04 and the individual fixed reflector heights for each data (given in the table) and OCS measurements, and estimation rates are given in Table 8. According to the results of P-04, the mean correlation values between amplitude and phase estimates and OCS measurements were 82.64% and 81.55%, respectively. The estimation rate was found as 95.61% on average. It is seen that there is no significant change in amplitude correlation and estimation rate in P-04 compared to P-03 analysis, and there is an increase of ~4% in phase correlation.

Table 8. Correlation percentage of P-04

Data ID	ρ (%)		ER (%)	Constant RH (m)
	A	φ		
S2_01	86.72	75.53	94.29	2.45
S2_02	76.57	78.12	93.33	2.54
S2_03	73.05	84.96	93.81	2.40
S2_04	84.72	83.16	93.33	2.47
S2_05	88.63	85.48	92.86	2.42
S2_06	90.45	81.19	96.19	2.61
S2_07	62.31	79.67	93.33	2.27
S2_08	92.00	91.61	99.05	2.56
S2_09	74.31	71.99	93.33	2.43
S2_10	71.70	87.95	100.00	2.47
S2_11	88.27	73.57	98.10	2.40
S2_12	79.40	83.39	100.00	2.41
S2_13	87.47	83.68	97.62	2.45
S2_14	89.44	77.17	93.33	2.46
S2_15	82.23	84.53	94.29	2.43
S2_16	89.31	89.91	98.10	2.41
S2_17	87.11	79.33	93.33	2.14
S2_18	94.75	89.33	99.52	2.47
S2_19	68.34	79.47	93.33	2.62
S2_20	90.42	86.77	94.29	2.59
S2_21	90.32	65.11	100.00	2.40
S2_22	70.47	82.22	91.90	2.60
Mean	82.64	81.55	95.61	

The overall results obtained from these four different processes can be found in Table 9 in terms of correlation and estimation rates. It is found that only amplitude estimates have a high correlation in P-01 and P-02, and the phase and reflection depth estimates did not give good results. In P-01 and P-02, the reflector heights are estimated daily, which change everyday. Thus, phase estimations were found meaningless. In P-03 and P-04, it is seen that both amplitude and phase estimations give highly correlated results with OCS measurements.

Table 9. Overall Results with estimations

Data ID	ρ (%)						ER (%)			
	P-01	P-02	P-03		P-04		P-01	P-02	P-03	P-04
	A	A	A	φ	A	φ				
S2_01	91.31	89.58	86.72	75.53	86.72	75.53	85.24	93.33	94.29	94.29
S2_02	74.60	77.63	75.92	63.99	76.57	78.12	42.86	90.48	93.33	93.33
S2_03	75.99	79.35	75.04	85.80	73.05	84.96	50.48	86.19	93.81	93.81
S2_04	84.26	88.39	85.55	83.12	84.72	83.16	42.38	90.48	93.33	93.33
S2_05	89.03	94.43	87.07	86.63	88.63	85.48	55.24	90.48	92.86	92.86
S2_06	84.78	90.70	89.00	79.72	90.45	81.19	36.19	93.81	96.67	96.19
S2_07	56.59	88.06	56.61	84.59	62.31	79.67	12.38	51.43	93.33	93.33
S2_08	88.82	91.70	92.66	87.37	92.00	91.61	77.14	98.57	99.52	99.05
S2_09	81.99	75.76	75.25	73.08	74.31	71.99	8.10	73.81	93.33	93.33
S2_10	74.19	71.81	71.92	86.83	71.70	87.95	73.81	99.52	100.00	100.00
S2_11	76.57	87.61	86.11	76.75	88.27	73.57	56.19	85.71	98.57	98.10
S2_12	29.29	78.30	78.89	83.44	79.40	83.39	30.48	90.00	100.00	100.00
S2_13	64.16	87.33	87.47	83.68	87.47	83.68	42.38	84.29	97.62	97.62
S2_14	85.15	89.33	89.47	77.63	89.44	77.17	68.57	92.38	93.33	93.33
S2_15	88.37	88.22	81.71	83.62	82.23	84.53	86.67	93.33	94.29	94.29
S2_16	90.14	89.36	88.71	90.61	89.31	89.91	93.33	98.10	98.10	98.10
S2_17	82.18	85.76	86.70	-	87.11	79.33	43.81	91.90	92.86	93.33
S2_18	92.90	95.40	94.67	88.82	94.75	89.33	71.43	97.62	100.00	99.52
S2_19	77.45	81.90	70.11	51.95	68.34	79.47	60.95	92.38	93.81	93.33
S2_20	84.93	91.32	88.02	70.59	90.42	86.77	60.00	93.33	94.76	94.29
S2_21	73.52	87.82	89.43	66.61	90.32	65.11	42.38	77.62	100.00	100.00
S2_22	54.09	72.11	75.60	73.79	70.47	82.22	38.10	85.24	91.90	91.90
Mean	77.29	85.54	82.39	78.77	82.64	81.55	53.55	88.64	95.71	95.61

The graphical representations of the overall results in terms of correlation coefficient and estimation rates are represented in Figures 2 and 3, respectively. Moreover, the highest correlation value was obtained in P-02 amplitude estimates (95.40%, see Figure 4) and the lowest correlation values were obtained in P-01 amplitude estimates (29.29%). The highest estimation rate was found in P-03 (95.71%) and the lowest estimation rate was in P-01 (53.55%). The relationship between the data with the highest correlation in GPS-IR soil moisture estimates and OCS measurements can be seen in Figure 4.

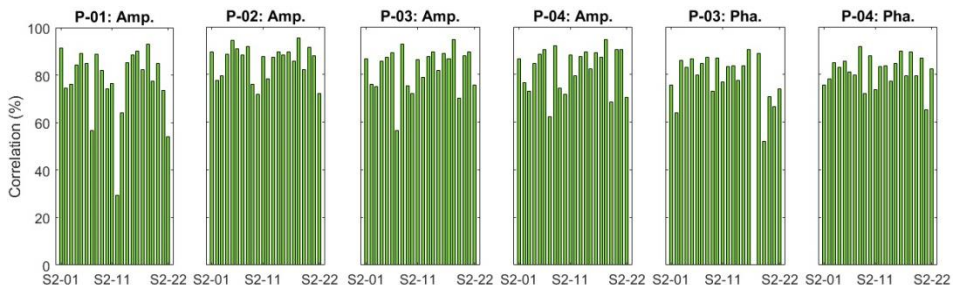


Figure 2. Correlation coefficients of all processing strategies (%)

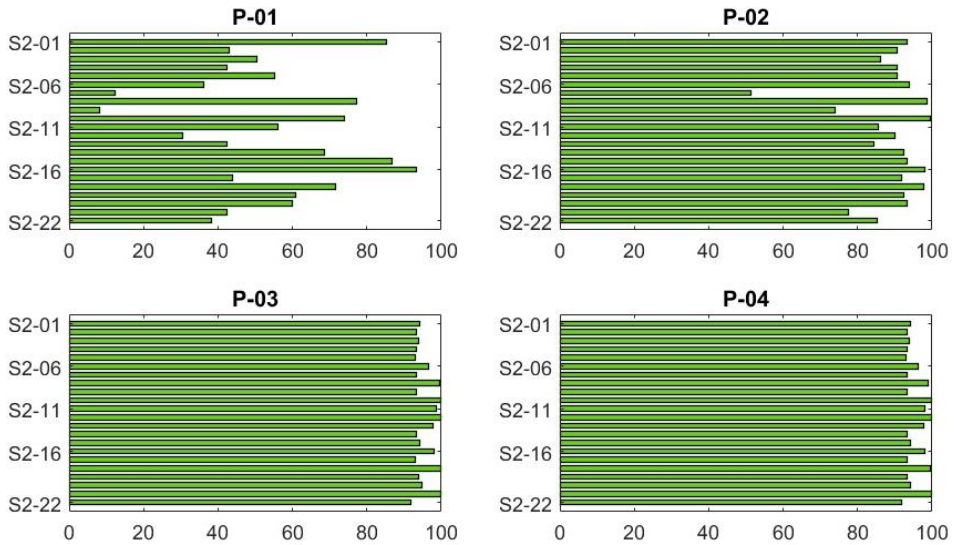


Figure 3. Estimation rates of the parameterization used (%)

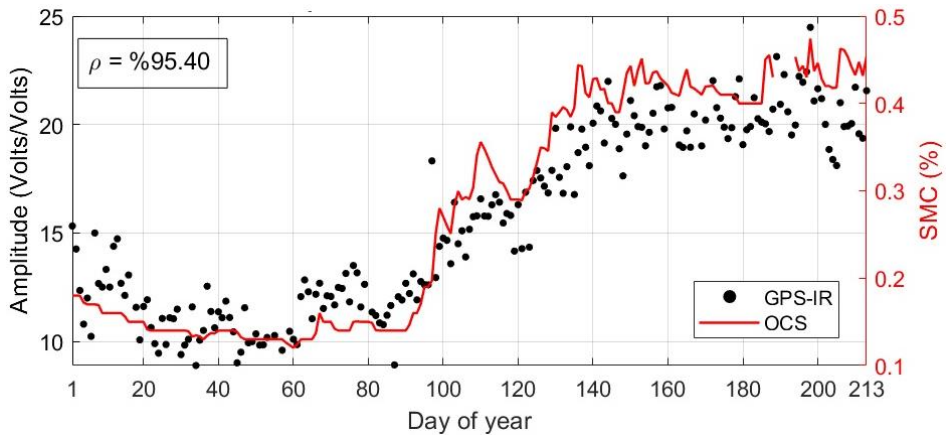


Figure 4. 7-month amplitude estimates obtained with the P-02 analysis of the G24 satellite data and soil moisture measurements at OCS (ρ denotes correlation coefficient)

5. CONCLUSION

The SNR data collected from OSOR GPS station for a 213-day period were evaluated to estimate the SMC with respect to the GPS reflectometry approach by different analyzing strategies. Estimation performances in terms of SNR-derived interferogram metrics (amplitude, phase and reflector height) generated from the GPS-IR methodology were established by the in-situ measurements, recorded at the OROMO station, which was nearby the OSOR station. Among four strategies, the P-02, where the reflector height was estimated daily by using LSP, and the amplitude and phase components were estimated with the LSE method with selecting the strong reflections as a condition of being three times greater than background noise, shows well agreement with in-situ measurements with 95% correlation. It can be concluded that this strategy

covers the most sensitive condition for estimation performance of soil moisture. Although estimations of phase and reflector height do not provide effective results, the amplitude estimations of the SNR data match with the SMC recorded. Moreover, the results show that the GPS-IR method provides high correlated outcomes; however, some parameters such as the slope of the study area, roughness of the surface, vegetation type should also be included in the future researches. Worldwide soil moisture measurements are crucial for many fields especially water cycles, climate change analyses, drought estimation, agriculture, etc. Therefore, the establishment of accurate and continuous observation systems will help to manage these facilities for the future planning stages.

Acknowledgement

We would like to thank Eric Kendrick and UNAVCO for providing the station photo and GNSS data. We would also like to thank Laboratory for Analysis of the Biosphere - University of Chile for providing soil moisture data. We are also grateful to the anonymous reviewers for their valuable comments. Figure 1c was plotted by using Generic Mapping Tools [21].

REFERENCES

- [1] Jackson, T., Schmugge, J., Engman, E. (1996). Remote sensing applications to hydrology: soil moisture. *Hydrological Sciences*, 41(4): 517-530.
- [2] Larson, K.M., Small, E.E., Gutmann, E.D., Bilich, A.L., Braun, J.J. and Zavorotny, V.U. (2008). Use of GPS receivers as a soil moisture network for water cycle studies. *Geophysical Research Letters*, Vol. 35, L24405, doi:10.1029/2008GL036013.
- [3] Larson, K.M., Small, E.E., Gutmann, E.D., Bilich, A.L., Axelrad, P., Braun, B. (2008). Using GPS multipath to measure soil moisture fluctuations: initial results. *GPS Solutions*, 12:173–177, doi:10.1007/s10291-007-0076-6.
- [4] Jin, S., Komjathy, A. (2010). GNSS Reflectometry and Remote Sensing: New Objectives and Results. *Advances in Space Research*, 46, 111–117.
- [5] Tunalioglu, N., Dogan, A. H., Durdag, U. M. (2019). GPS sinyal gürültü oranı verileri ile kar kalınlığının belirlenmesi (in Turkish). *Jeodezi ve Jeoinformasyon Dergisi*, 6(1), 1-9.
- [6] Bilskie, J. (2001). Soil water status: content and potential. Campbell Scientific, Inc. App. Note: 2S-1 <http://s.campbellsci.com/documents/ca/technical-papers/soilh20c.pdf>.
- [7] Ocalan, T., Erdogan, B., Tunalioglu, N., Durdag, U.M. (2016). Accuracy investigation of PPP method versus relative positioning using different satellite ephemerides products near/under forest environment. *Earth Sciences Research Journal* 20 (4), D1-D9
- [8] Dogan, A.H., Tunalioglu, N., Erdogan, B., Ocalan, T. (2018). Evaluation of the GPS Precise Point Positioning technique during the 21 July 2017 Kos-Bodrum (East Aegean Sea) Mw 6.6 earthquake. *Arabian Journal of Geosciences*, 11: 775, <https://doi.org/10.1007/s12517-018-4140-z>
- [9] Hofmann-Wellenhof, B., Lichtenegger, H., Wasle, E. (2007). GNSS—global navigation satellite systems: GPS, GLONASS, Galileo, and more. Springer Science & Business Media.
- [10] Larson, K.M., Braun, J.J., Small, E.E., Zavorotny, V.U., Gutmann, E.D., and Bilich, A.L. (2010). GPS Multipath and Its Relation to Near-Surface Soil Moisture Content. *IEEE Journal of Selected Topics in Applied Earth Observations and Remote Sensing*, Vol. 3, No. 1, pp. 91-99, doi: 10.1109/JSTARS.2009.2033612.
- [11] Han, M., Zhu, Y., Yang, D., Chang, Q., Hong, X., and Song, S. (2020). Soil moisture monitoring using GNSS interference signal: proposing a signal reconstruction method. *Remote Sensing Letters*, 11:4, 373-382, DOI: 10.1080/2150704X.2020.1718235

- [12] Larson, K. M., Small, E. E. (2016). Estimation of snow depth using L1 GPS signal-to-noise ratio data. *IEEE Journal of Selected Topics in Applied Earth Observations and Remote Sensing*, 9(10), 4802-4808
- [13] Roesler, C., Larson, K.M. (2018). Software tools for GNSS interferometric reflectometry (GNSS-IR). *GPS Solutions* (2018) 22:80, <https://doi.org/10.1007/s10291-018-0744-8>
- [14] Rodriguez-Alvarez, N, Bosch-Lluis, X., Camps, A., Aguasca, A., Vall-llossera, M., Valencia, E., Ramos-Perez, I., Park, H. (2011). Review of crop growth and soil moisture monitoring from a ground-based instrument implementing the interference pattern GNSS-R technique. *Radio Science*, vol. 46, no. 06, pp. 1-11, Dec. 2011, doi: 10.1029/2011RS004680.
- [15] Larson, K. M., Nievinski, F. G. (2013). GPS snow sensing: results from the EarthScope Plate Boundary Observatory. *GPS Solutions*, 17(1), 41-52.
- [16] Nievinski, F. G., Larson, K. M. (2014). Inverse modeling of GPS multipath for snow depth estimation-Part I: Formulation and simulations. *IEEE Transactions on Geoscience and Remote Sensing*, 52(10), 6555-6563.
- [17] Small, E. E., Larson, K. M., Chew, C. C., Dong, J., Ochsner, T. E. (2016). Validation of GPS-IR soil moisture retrievals: Comparison of different algorithms to remove vegetation effects. *IEEE Journal of Selected Topics in Applied Earth Observations and Remote Sensing*, 9(10), 4759-4770.
- [18] Ban, W., Yu, K., Zhang, X. (2017). GEO-satellite-based reflectometry for soil moisture estimation: Signal modeling and algorithm development. *IEEE Transactions on Geoscience and Remote Sensing*, 56(3), 1829-1838.
- [19] Martín, A., Ibáñez, S., Baixauli, C., Blanc, S., Anquela, A. B. (2020). Multi-constellation GNSS interferometric reflectometry with mass-market sensors as a solution for soil moisture monitoring. *Hydrology and Earth System Sciences*, 24(7), 3573-3582.
- [20] Swinscow, T.D.V., Campbell, M.J. (2002). *Statistics at square one*, 10th edn. BMJ Books. ISBN 0-7279-1552-5
- [21] Wessel, P., Smith, W.H.F. (1998). New improved version of Generic mapping tools released, *EOS Trans. AGU* 79 (47) 579.